An evaluation method of supercritical CO_2 thickening result for particle transporting

Lei Hou [a,b*], Tingxue Jiang [a], He Liu [c], Xueyu Geng [d] Baojiang Sun [e], Gensheng Li [b], Siwei Meng[c]
[a] SINOPEC Research Institute of Petroleum Engineering, Beijing 100101, China
[b] School of Petroleum Engineering, China University of Petroleum (Beijing), Beijing 102249, China
[c] PetroChina Research Institute of Petroleum Exploration and Development, Beijing 100083, China
[d] School of Engineering, The University of Warwick, Coventry CV4 7AL, UK
[e] School of Petroleum Engineering, China University of Petroleum (East China), 266580, China

Abstract

This paper aims to propose an evaluation method for measuring the supercritical CO_2 thickening result for particle transporting. By analyzing the particle transporting trajectory in supercritical CO_2, the cotangent of particle landing angle (ratio of particle horizontal velocity to vertical velocity) was proposed as a new criterion of thickening result. Previous studies of SC-CO_2 thickening were evaluated and drawn in three-dimensions using this new criterion. Moreover, the effects of CO_2 density and viscosity on particle vertical and horizontal velocities and the cotangent of particle landing angle were analyzed. The cotangent of particle landing angle is more sensitive to SC-CO_2 density than the vertical and horizontal viscosities. Therefore, supercritical CO_2 density should be considered for the evaluation of supercritical CO_2 thickening for particle transporting. The particle settling velocity was found to determine the particle transporting distance and also the transporting capability of supercritical CO_2. According to this conclusion, the apparatus for experimental evaluation of supercritical CO_2 thickening will be miniaturized significantly by simplification from two-dimensional velocities measurement into one direction, particle settling velocity in vertical direction. Additionally, the supercritical CO_2 viscosity was found to have an optimum value, increasing in line with improvements in viscosity as particle transportation flattened out.

Keywords: xxx

1. Introduction

Supercritical CO_2 (SC-CO_2) is an efficient and environmentally friendly petroleum engineering fluid, which has drawn great interest especially in the area of reservoir simulation [1]. SC-CO_2 fracturing fluid invades the tight and micro channels of the formation more easily than water-based fluids. The fracture network is more complicated and the simulated reservoir volume (SRV) is larger by SC-CO_2 fracturing [2,3]. SC-CO_2 has competitive adsorption with CH_4 and replaces the adsorbed natural gas. It is freely soluble in heavy oil and reduces the oil viscosity [4]. Additionally, SC-CO_2 inhibits clay expansion in the reservoir and reduces the skin factor near the wellhole [5,6]. Hence, the simulation result using SC-CO_2 is considerably greater than that using water-based fluid [7-9].

However, the low viscosity of SC-CO_2 is the key factor that restricts its widespread use, because the particle transporting capability of SC-CO_2 is relatively low and the volume of injected proppant by SC-CO_2 during the fracturing is limited. The most recent application of SC-CO_2 fracturing by PetroChina in Jilin Oilfield showed that the sand concentration transported by SC-CO_2 was merely 5.3 %–6.4%, which was less than half of the sand ratio when water-based fluid was utilized [10]. Therefore, the SC-CO_2 thickening is one of most urgent issues needed to be solved.

Plenty of SC-CO_2 thickening research work has been conducted in order to enhance its particle transporting capability [11-13]. The organic silicone polymer and fluoropolymer are considered a good thickener for SC-CO_2. 6% PDMS, assisted by 20% methylbenzene, can enhance the SC-CO_2 viscosity 90 times, up to 3.48 mPa·s [14,15]. However, the current thickening research has two main insufficiencies for the SC-CO_2 fracturing and particle transportation:

(i) *The lack of evaluation method for SC-CO_2 thickening result.*

There is no evaluation method that can reflect the SC-CO_2 thickening result in the form of particle transporting capability. The thickening research work has an impending demand for a more specific target of thickened viscosity and density values that are large enough for efficient particle transporting. By supplementing this deficiency, SC-CO_2 thickening work will become more efficient.

(ii) *The neglect of effect of SC-CO_2 density on particle transporting*.

The viscosity of SC-CO_2 is the main parameter that thickening research concerns [Ref]. However, studies on particle settling and flowing in SC-CO_2 indicated that the density of SC-CO_2 also had significant effects on its particle transporting capability [Ref]. The value of the particle settling velocity in SC-CO_2 was found to be closer to the value in liquid than the value in gas [Ref]. The slippage velocity and displacement between particle and SC-CO_2 were also more sensitive to SC-CO_2 density than its viscosity. Therefore, the impact of enhanced SC-CO_2 density on particle transporting improvement needs to be evaluated.

This paper aimed to solve these two key issues mentioned above. A new evaluation method was proposed to provide a reference for SC-CO_2 thickening research. The current SC-CO_2 thickening results were appraised by the new criterion. The effect of SC-CO_2 density on particle motion in both vertical and horizontal directions was analyzed by particle motion model, and compared with the effect of SC-CO_2 viscosity.

2. Numerical methods

2.1 Particle motion models in vertical and horizontal directions in SC-CO_2

Previous studies have proposed the particle motion models in SC-CO_2 [16,17]. Both of the models were verified to be accurate by experiments and were also qualified by numerical analyses. In this paper, the calculation of particle-SC-CO_2 two phase flow will be applied for evaluating SC-CO_2

thickening results. The particle settling velocity calculation in SC-CO_2 is

$$\begin{cases} \upsilon_{\infty} = \dfrac{\mu}{\rho_f d_p}[0.1196(\dfrac{\rho_p}{\rho_f})^2 - 0.1216\dfrac{\rho_p}{\rho_f} - 0.2961]Ar^{[-0.214\ln(\frac{\rho_p}{\rho_f})+0.8241]} \\ Ar = \dfrac{g(\rho_p - \rho_f)\rho_f d_p^{\ 3}}{\mu^2} \end{cases} \quad (1)$$

where υ_{∞} is the particle settling velocity, ρ_f is the density of SC-CO_2, μ is the viscosity of SC-CO_2, ρ_p is the density of particles, d_p is the diameter of the particle, Ar is particle's Archimedes number, g is the ….

The particle horizontal velocity following with SC-CO_2 is calculated by

$$\begin{cases} \upsilon_p = \upsilon_f - \dfrac{T_r \cdot \upsilon_f}{t \cdot \upsilon_f + T_r} \\ T_r = \dfrac{2d_p(2\rho_p + \rho_f)}{3\rho_f C_D} \\ C_D = \dfrac{4g(\rho_p - \rho_f)d_p}{3\upsilon_{\infty}^2 \rho_f} \end{cases} \quad (2)$$

where υ_p is the particle horizontal velocity, υ_f is the SC-CO_2 flowing velocity, T_r is the procedure parameter, C_D is the drag coefficient.

2.2 The new evaluation method of SC-CO_2 thickening result

During the field fracturing operation, SC-CO_2 fracturing fluid has a primary mission to carry the proppant particles into fractures as deeply as possible. The purpose of SC-CO_2 thickening is to enhance its particle transporting capability. The slower the particle settles vertically and the faster the particle flows horizontally, the further the particle can be transported into the fracture. Therefore, particle velocities in vertical and horizontal directions will be used to evaluate the SC-CO_2 thickening result. Experimental research further revealed particle transporting behavior in SC-CO_2. The particle tracks under four different SC-CO_2 conditions are shown in Figure 1. The dashed lines are particle motion tracks that are all straight. This indicate that the vertical and horizontal velocities of particle are constant. Previous studies found that the particles experienced a very short acceleration before they kept a constant velocity flowing with SC-CO_2 [16,17]. The different locations of particles might be caused by the interactions between particles when they first entered into the experimental apparatus. After that, they flowed with SC-CO_2 freely and exhibited constant velocities. The specific particle parameters are listed in Table 1.

Apparently, most of the particle tracks form practically the same angles relative to the horizon in each group of experiments, which mean that the particles in each group will strike the bottom with the same landing angle. When particles have the same densities and diameters, the cotangent of landing angles (ratios of particle horizontal velocities to vertical velocities) are practically the same. Consequently, the cotangent of particle landing angle (cot(α)) in SC-CO_2 is proposed as the new criterion for evaluating SC-CO_2 thickening result. The larger the cotangent α is, the deeper the particle can be carried into the fracture and the better the SC-CO_2 thickening result is.

Based on Eqs. (1) and (2), the equation for cotangent α is

$$\cot\alpha = \upsilon_p / \upsilon_\infty \tag{3}$$

Combining with Eqs. (1) and (2), cot(α) can be calculated and the SC-CO_2 thickening result can be evaluated.

2.3 Numerical description of particle transporting in SC-CO_2

To illustrate the cotangent of landing angle (cot(α)) further, the particle transportation under experimental condition (the Exp. (d) is taken as an example) was numerically descripted by using the integral forms of Eqs. (1) and (2), which are

$$\begin{cases} \frac{\pi d_p^3}{6}\rho_p\frac{d\upsilon_p}{dt}=-\frac{\pi d_p^2}{8}\rho_f\upsilon_p^2C_d+\frac{\pi d_p^3}{6}(\rho_p-\rho_f)g+\frac{\pi d_p^3}{12}\rho_f(\frac{d\upsilon_f}{dt}-\frac{d\upsilon_p}{dt})+\frac{3d_p^2}{2}(\pi\rho_f\mu)^{1/2}\int_0^t\frac{\frac{d\upsilon_f}{dt}-\frac{d\upsilon_p}{dt}}{\sqrt{t-\tau}}d\tau \\ \frac{\pi d_p^3}{6}\rho_p\frac{d\upsilon_p}{dt}=-\frac{\pi d_p^2}{8}\rho_f(\upsilon_f-\upsilon_p)^2C_d+\frac{\pi d_p^3}{12}\rho_f(\frac{d\upsilon_f}{dt}-\frac{d\upsilon_p}{dt})+\frac{3d_p^2}{2}(\pi\rho_f\mu)^{1/2}\int_0^t\frac{\frac{d\upsilon_f}{dt}-\frac{d\upsilon_p}{dt}}{\sqrt{t-\tau}}d\tau \\ C_d=\frac{4g(\rho_p-\rho_f)d_p}{3\rho_f v_\infty^2} \\ v_\infty=\frac{\mu}{\rho_f d}[0.1196(\frac{\rho_p}{\rho_f})^2-0.1216\frac{\rho_p}{\rho_f}-0.2961]Ar^{[-0.214\ln(\frac{\rho_p}{\rho_f})+0.8241]} \end{cases} \tag{4}$$

Three assumptions were proposed to simplify the calculation. Firstly, the rotation effect on particle motion was ignored because the particle sphericity was good, although the rotation was hard to measure based on the 2D pictures. Secondly, particle interaction was the only factor that resulted in three parallel particle trajectories. Lastly, impact of particles happened at a time (T) and changed the particle velocity only in the vertical direction.

Based on these assumptions, particles entered the fracture from the original point in Figure 2. At the T moment, particle 1 and particle 3 had an impact that slowed particle 1 and accelerated particle 3 both in the vertical directions. The particle 2 was uninfluenced during the impact. Due to the action of gravity and friction, particle 1 and particle 3 experienced an acceleration and deceleration separately in the vertical direction and then achieved the equilibrium. Eventually, these particles were transported in uniform linear motion, as shown in Figure 2.

The experimental observation in Figure 1 (d) showed parts of the particle tracks and was integrated into Figure 2. The dotted circle represented the observation window. The window's diameter and positions of the windows and the particle inlet were drawn by reducing a certain proportion of the actual experimental setup. Apparently, the numerical particle tracks coincided with the trajectories captured in the observation window during the experiment. The three particles settled down to the bottom with the same landing angle. The calculated horizontal transporting distances of the particles were 0.278m, 0.254 m and 0.231m, respectively.

3. Results and discussion

The particle parameters for numerical analysis were optimized according to the commonly used proppant for the fracturing operation. The proppant particle diameter and density are 0.5 mm and 2800 kg/m^3 respectively, which are average diameter and density of conventional proppant. The reference value of SC-CO_2 flow rate is 1 m/s based on the common field pump rates and fracture sizes [18]. The density and viscosity of SC-CO_2 were taken from the National Institute of Standards and Technology website from USA [19]. The reference values of SC-CO_2 density and viscosity are 763.68 kg/m^3 and 0.068 mPa·s respectively, which are close to the underground conditions at a depth of 2000 – 3000 m during the fracturing operation [20,21].

3.1 Effects of SC-CO_2 density and viscosity on particle motion in vertical direction

The effect of SC-CO_2 density on particle motion in vertical direction is shown in Figure 3. The vertical velocity declines with the increasing of SC-CO_2 density in the way of logarithmic function. Meanwhile, vertical velocity decreases with the increase of SC-CO_2 viscosity in terms of of power function, as shown in Figure 4. Generally, the SC-CO_2 density more evenly impacts than the viscosity does. The reducing tendency of the curve approximates to a straight line in Figure 3. However, in Figure 4, the viscosity-enhancing slows down the vertical velocity sharply at the very beginning. After 0.001 Pa·s, the dropping tendency becomes less pronounced and the viscosity-enhancing effects on vertical velocity tended to be mild. The decrease range is another significant difference. The vertical velocity drops by approximately 75%, determoned by SC-CO_2 density. On the other hand, an increased viscosity of SC-CO_2 reduces the vertical velocity by less than 50%.

3.2 Effects of SC-CO_2 density and viscosity on particle motion in horizontal direction

The horizontal velocity increases with the increase of SC-CO_2 density and viscosity, as shown in

Figure 5 and Figure 6. Similar with the vertical velocity variation tendencies, the horizontal velocity increases with increasing SC-CO_2 density in the way of logarithmic function, and increases with the increasing of SC-CO_2 viscosity in the way of power function. However, the amplitude of horizontal velocity variation is much less than the amplitude of vertical velocity variation. Above all, the horizontal velocities under various SC-CO_2 densities and viscosities are closed to the SC-CO_2 flow rate. Thus, the horizontal velocity has a less important role for particle transporting than the vertical velocity does. In other words, the particle settling velocity determines the particle transporting distance and also the transport capability of SC-CO_2. This conclusion is extremely useful because the experimental evaluation of the resultant SC-CO_2 thickening for particle transporting is simplified from two-dimensional velocities measurement to one dimensional measurement. The steady flow circulation of pure SC-CO_2 for two-dimensional velocities measurement needs CO_2 phase transformation from liquid (in the storage tanks) to supercritical (during the particle-CO_2 two-phase flow) and then cooled back into liquid. This circulation takes more than 1000 square foot room for pumps, heater, cooler, tanks, pipes and other necessary equipment [22,23]. For thickened SC-CO_2, the flow circulation is even impossible for the rinse problem in the circulation. Nevertheless, this simplification from two-dimensional velocities measurement to one dimension will miniaturize the apparatus significantly.

3.3 Effects of SC-CO_2 density and viscosity on cot(α)

The cot(α) increases around 3 times (from 3.15 to 9.09) with the SC-CO_2 density rose up to 5 times (from 200 kg/m^3 to 1000 kg/m^3), as shown in Figure 7. On the other hand, cot(α) increases less than 2 times (from 4.63 to 8.27) with the SC-CO_2 viscosity enhanced up to 500 times (from 0.00001 Pa·s to 0.005 Pa·s), as shown in Figure 8. Apparently, cot(α) is more sensitive to SC-CO_2 density than viscosity. Therefore, the density of SC-CO_2, rather than only the viscosity, should be considered for the evaluation of SC-CO_2 thickening results.

The SC-CO_2 viscosity has more unevenly impacts on cot(α) than the density. Similar patterns have been found from Figure 3 to Figure 6. The effects of SC-CO_2 viscosity usually are significant at the early stage of its increasing and gradually flatten out during the later period. According to this revelation, there is an optimum value of enhanced SC-CO_2 viscosity. After the SC-CO_2 thickening exceeds the optimum value, the increasing of viscosity has less impact on particle transporting. Under the computational conditions of proppant, SC-CO_2 flow and density in this study, the optimum value of enhanced SC-CO_2 viscosity is about 0.001 Pa·s.

3.4 Evaluation of SC-CO_2 thickening results using the new method

The synthetic effects of SC-CO_2 density and viscosity on particle transporting based on cot(α) have been drawn in three-dimensional diagram in Figure 9 and Figure 10. In particular, the SC-CO_2 thickening results are evaluated based on its particle transporting capability (cot(α)) rather than the magnification of SC-CO_2 viscosity. The previous studies of SC-CO_2 thickening, Fellclano [24] and Siwei [10], have been used and compared with the original SC-CO_2 parameters. The lower smooth line on the left represents the particle cot(α) under the original SC-CO_2 density and viscosity. The higher broken line on the right represents the cot(α) based on the SC-CO_2 thickening result.

The impacts of enhanced SC-CO_2 density and viscosity on particle transportation based on cot(α) are clearly shown in Figure 9 and Figure 10. The curves are folded up with the increasing of enhanced SC-CO_2 density and viscosity. It is more distinctly in Figure 10 that cot(α) is more sensitive to enhanced SC-CO_2 density. Because the effect of SC-CO_2 viscosity on cot(α) after 100 times increasing becomes more and more moderate, as shown in Figure 8. In some cases in Figure 10, the combined impacts of increasing density and decreasing viscosity result in the rising of particle cot(α). However, the improvement of particle transportation due to the increasing of SC-CO_2 viscosity is significant by contrasting Figure 9 and Figure 10. The particle cot(α) under the same SC-CO_2 density increases by 32% to 57% with the SC-CO_2 viscosity increased by approximately 40 times (Figure 9 and Figure 10).

4. Conclusions

In this work, the numerical evaluation method of SC-CO_2 thickening result was studied to reveal its particle transporting improvement. The cotangent of particle landing angle (ratio of particle horizontal velocity to vertical velocity) was proposed as a new criterion based on the particle vertical and horizontal motion in SC-CO_2. The larger the cotangent of particle landing angle (cot(α)) is, the further the particle can be carried and the better the SC-CO_2 thickening result is. The previous studies of SC-CO_2 thickening were evaluated and drawn in three-dimensional diagram using the new criterion. Further analyses indicated that the particle settling velocity determined the particle transporting distance and also the transporting capability of SC-CO_2. According to this conclusion, the apparatus for experimental evaluation of SC-CO_2 thickening will be miniaturized significantly by the simplification from two-dimensional velocities measurement to one direction (particle settling velocity in vertical direction). The SC-CO_2 density was found to have important effects on particle transporting and should be considered for the evaluation of SC-CO_2 thickening results. The SC-CO_2 viscosity was found to have an optimum value, exceeding which the impact of viscosity on particle transporting trended to be gentle.

Acknowledgements

Research supported by the National Natural Science Foundation of China (Project No. 51490653).

References

[1] R. Khanpour, M.R. Sheikhi-Kouhsar, F. Esmaeilzadeh, Removal of contaminants from polluted drilling mud using supercritical carbon dioxide extraction, J. Supercritical Fluids 88 (2014) 1–7.

[2] X. Li, D. Elsworth, Geomechanics of CO_2 enhanced shale gas recovery, J. Natural Gas Science & Engineering 26 (2014) 1607–1619.

[3] L. Ribeiro, H. Li, J. Bryant, Use of a CO_2–hybrid fracturing design to enhance production from unpropped–fracture networks, SPE Production & Operations Preprint (2016).

[4] T. Wu, Q. Xue, X. Li, Y. Tao, Y. Jin, C. Ling, S. Lu, Extraction of kerogen from oil shale with supercritical carbon dioxide: molecular dynamics simulations, J. Supercrit. Fluids 107 (2016) 499–506.

[5] Y.X. Cheng, G.S. Li, H.Z. Wang, Z.H. Shen, S.C. Tian, X. Fan, Pressure boosting effect in perforation cavity during supercritical carbon dioxide jet fracturing, Atomization and Sprays 23 (2013) 463–474.

[6] A. Haghtalab, H.S. Panah, Modeling cloud point of soluble polymers in supercritical carbon dioxide fluid using PCP-SAFT equation of state – an application in enhanced oil recovery, J. Supercritical Fluids 97 (2015) 45–50.

[7] M.L. Sinal, G. Lancaster, Liquid CO2 fracturing: advantages and limitations, J. Canadian Petroleum Technology 26 (1987) 26–30.

[8] R. Tudor, A. Poleschuk, Low-viscosity, low-temperature fracture fluids, J. Canadian Petroleum Technology 35 (1996) 31–36.

[9] G. Zhang, C. Taberner, L. Cartwright, T. Xu, Injection of supercritical CO2 into deep saline carbonate formations: predictions from geochemical modeling, SPE J. 16 (2011) 959–967.

[10] S. Meng, H. Liu, J. Xu, Y. Duan, Q. Yang, Z. Yao, Optimisation and performance evaluation of liquid CO_2 fracturing fluid formulation system, Perth, 25–27 October, in: Proceedings of the SPE Asia Pacific Oil & Gas Conference and Exhibition, 2016.

[11] C. Shi, Z. Huang, E. Beckman, R. Enick, S. Kim, D. Curran, Semi-fluorinated trialkyltin fluorides and fluorinated telechelic ionomers as viscosity-enhancing agents for carbon dioxide, Ind. Eng. Chem. Res 40 (2001) 908–913.

[12] J. Xu, A. Wlaschin, R. M. Enick, Thickening CO2 with the fluoroacrylate-styrene copolymer, SPE J. 8 (2003) 85–91.

[13] X. Luo, S. Wang, Z. Wang, Z. Jing, M. Lv, Z. Zhai, T. Han, Experimental investigation on rheological properties and friction performance of thickened CO_2 fracturing fluid, J. Petroleum Science and Eng. 133 (2015) 410–420.

[14] J. H. Bae, C. A. Irani, A laboratory investigation of viscosified CO_2 process: the thickened CO_2 process utilizing a commercial silicon polymer and toluene as cosolvent is technically viable, SPE Advanced Technology Series 1 (1993) 166–171.

[15] L. L. Williams, J. B. Rubin, H. W. Edwards, Calculation of Hansen Solubility Parameter Values for a Range of Pressure and Temperature Conditions, Including the Supercritical Fluid Region, Industrial & Engineering Chemistry Research 43 (2004) 4967–4972.

[16] L. Hou, B. Sun, Z. Wang, Q. Li, Experimental study of particle settling insupercritical carbon dioxide, J. Supercrit. Fluids 100 (2015) 121–128.

[17] L. Hou, B. Sun, X. Geng, T. Jiang, Z. Wang, Study of the slippage of particle/supercritical

CO2 two–phase flow, J. Supercritical Fluids 120 (2017) 173–180.

[18] J. Micheal, Economides, in: Reservoir Stimulation, 3rd ed., Petroleum IndustryPress, Beijing, 2002, pp. 145–151.

[19] National Institute of Standards and Technology, Chemistry WebBook, NIST,2014 http://webbook.nist.gov/chemistry/fluid/.

[20] N.C. Dutta, Geopressure prediction using seismic data: Current status and theroad ahead, Geophysics 67 (2002) 2012–2041.

[21] S. Cao, I. Lerche, Geohistory, thermal history and hydrocarbon generationhistory of Navarin Basin COST No.1 well Bering Sea Alaska, J. Petrol. Geol. 12(1989) 325–352.

[22] Y.K. Du, R.H. Wang, H.J. Ni, H.J. Huo, Z.Y. Huang, W.M. Yue, H.X. Zhao, B. Zhao,Rock-breaking experiment with supercritical carbon dioxide jet, J. Chin. Univ.Petrol. 36 (2012) 93–96.

[23] Y. Du, R. Wang, H. Ni, M. Li, W. Song, H. Song, Determination of rock-breakingperformance of high-pressure supercritical carbon dioxide jet, J.Hydrodynam. B 24 (2012) 554–560.

[24] F. M. Liave, F. TH. Chung, T. E. Burchfield, Use of entrainers in improving mobility control of supercritical CO_2, 1 (1990) 47–51.

Fig. 1. The particle tracks under different SC-CO_2 conditions. (a) The temperature, pressure and flow rate of SC-CO_2 are 45.9 °C, 8.89 MPa and 1.13 m/s, respectively. (b) The temperature, pressure and flow rate of SC-CO_2 are 46.7 °C, 9.52 MPa and 1.28 m/s, respectively. (c) The temperature, pressure and flow rate of SC-CO_2 are 47.5 °C, 10.91 MPa and 1.15 m/s, respectively. (d) The temperature, pressure and flow rate of SC-CO_2 are 45.9 °C, 10.96 MPa and 1.08 m/s, respectively.

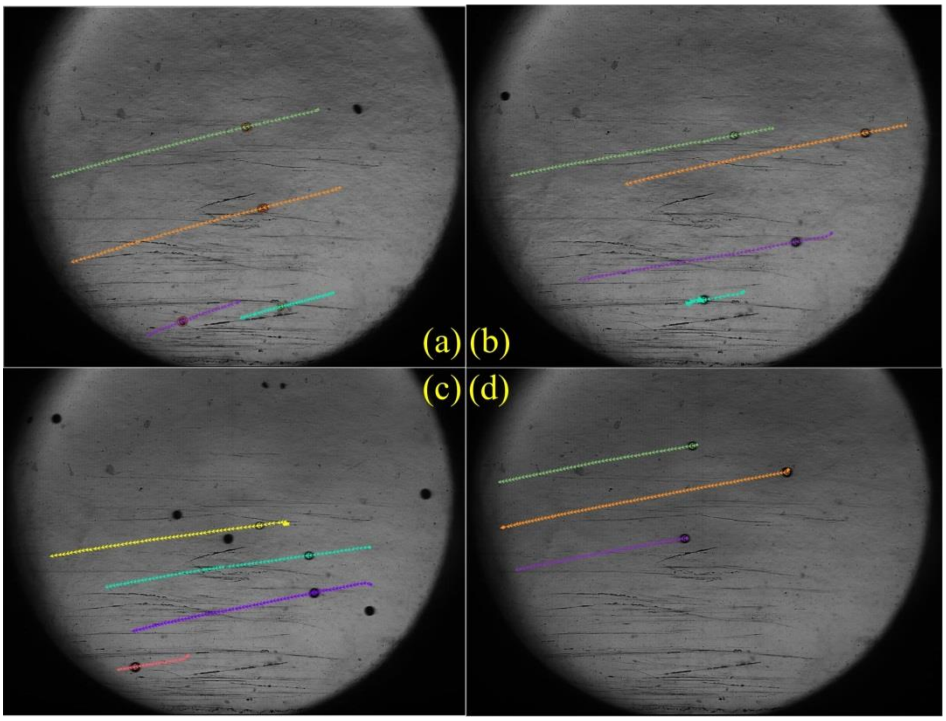

Fig. 2. The numerical description of particle transporting in SC-CO_2 under the conditions of 45.9 °C, 10.96 MPa and 1.08 m/s.

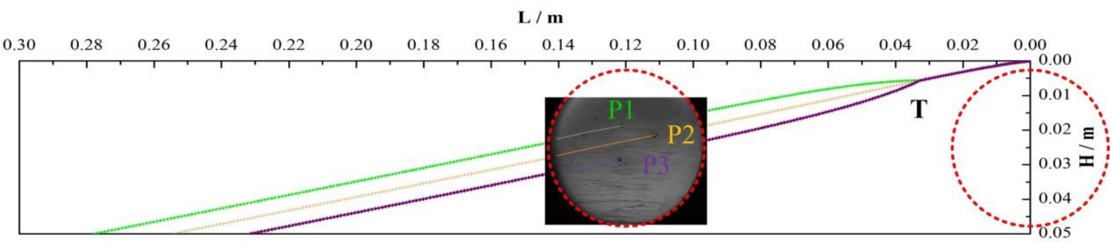

Fig. 3. The effect of SC-CO_2 density on particle vertical velocity. The SC-CO_2 viscosity is 0.068 mPa·s. The particle diameter and density are 0.5 mm and 2800 kg/m^3 respectively.

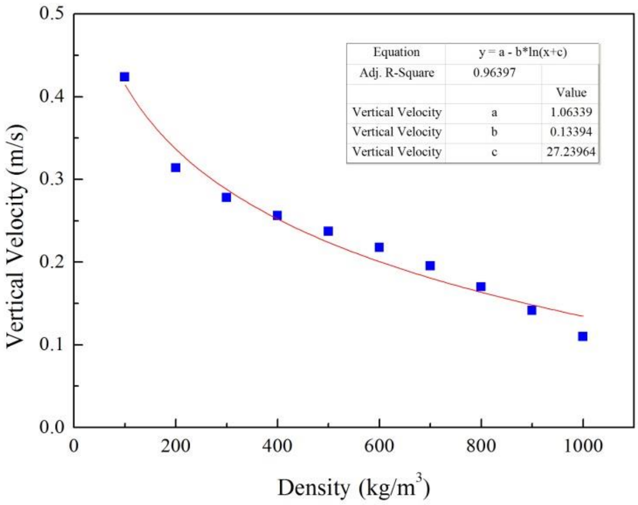

Fig. 4. The effect of SC-CO_2 viscosity on particle vertical velocity. The SC-CO_2 density is 763.68 kg/m^3. The particle diameter and density are 0.5 mm and 2800 kg/m^3 respectively.

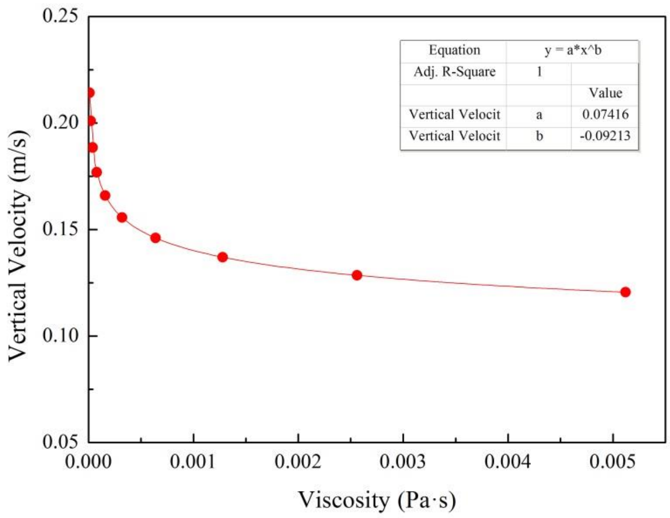

Fig. 5. The effect of SC-CO_2 density on particle horizontal velocity. The SC-CO_2 viscosity is 0.068 mPa·s. The particle diameter and density are 0.5 mm and 2800 kg/m^3 respectively.

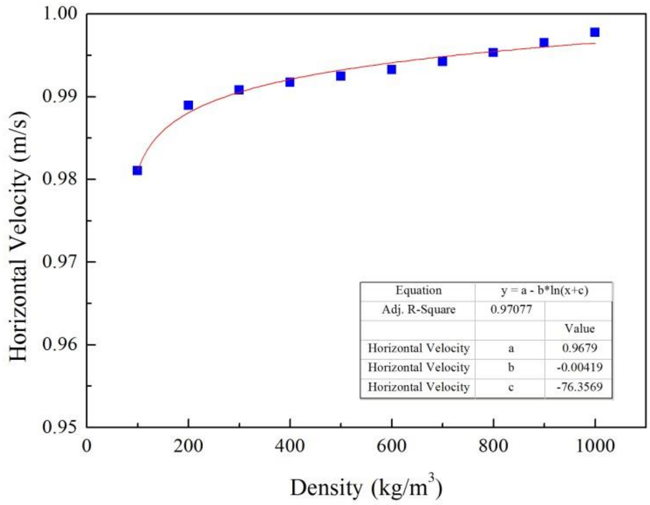

Fig. 6. The effect of SC-CO_2 viscosity on particle horizontal velocity. The SC-CO_2 density is 763.68 kg/m^3. The particle diameter and density are 0.5 mm and 2800 kg/m^3 respectively.

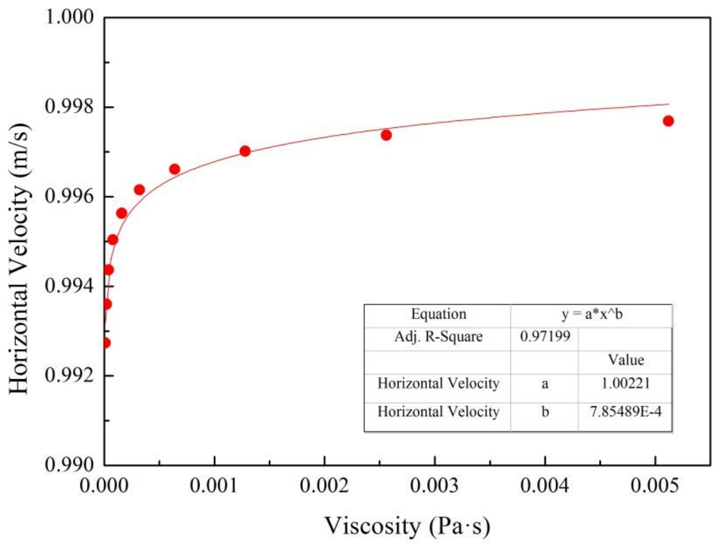

Fig. 7. The effect of SC-CO_2 density on cotangent of particle landing angle (cot *α*) . The SC-CO_2 viscosity is 0.068 mPa·s. The particle diameter and density are 0.5 mm and 2800 kg/m^3 respectively.

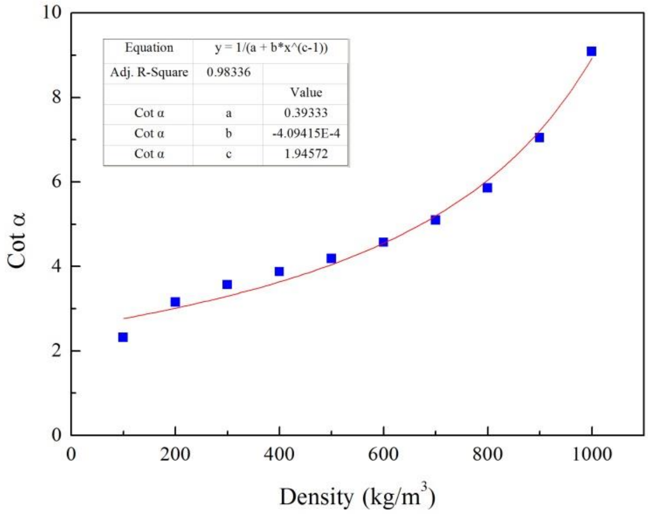

Fig. 8. The effect of SC-CO_2 viscosity on cotangent of particle landing angle (cot *α*) . The SC-CO_2 density is 763.68 kg/m^3. The particle diameter and density are 0.5 mm and 2800 kg/m^3 respectively.

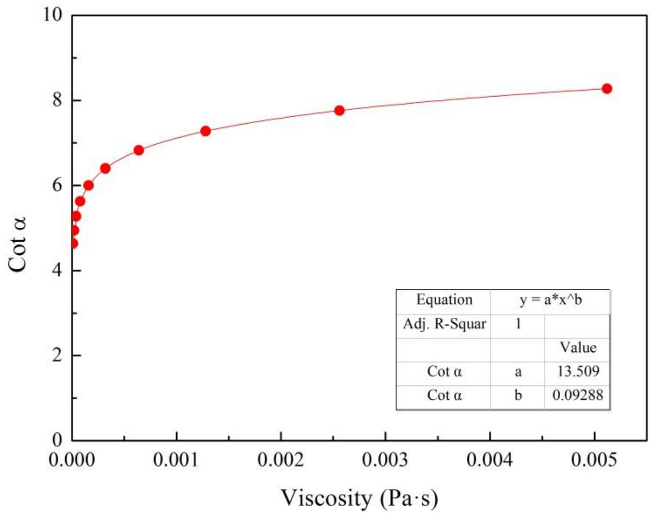

Fig. 9. The evaluation of SC-CO_2 thickening result by Fellclano [24] using the cot *α* method. The particle diameter and density are 0.5 mm and 2800 kg/m^3 respectively.

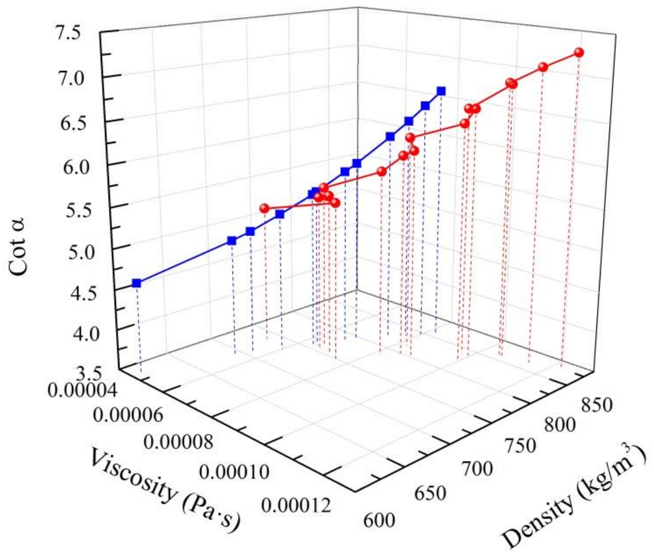

Fig. 10. The evaluation of SC-CO_2 thickening result by Siwei [10] using the cot *α* method. The particle diameter and density are 0.5 mm and 2800 kg/m^3 respectively.

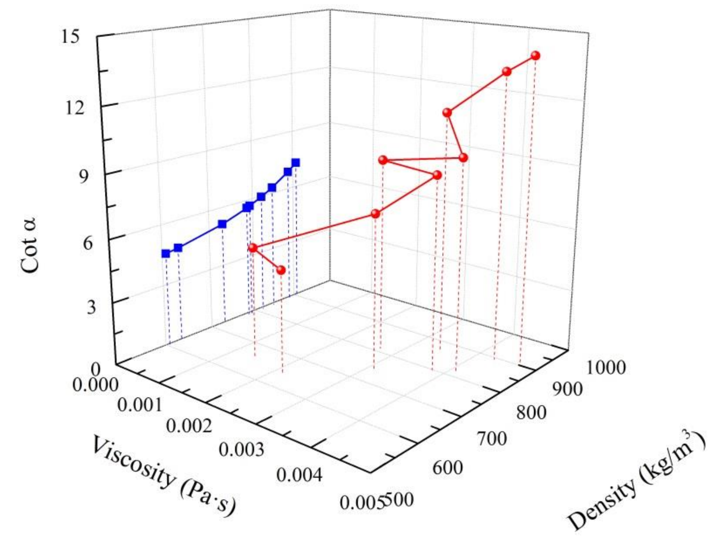

Table 1 The particle measured vertical and horizontal velocities under different conditions.

	Temperature (°C)	Pressure (MPa)	Flow rate (m/s)	υ_x (m/s)	υ_y (m/s)	υ_x/υ_y (cot(α))
Exp. (a)	45.9	8.89	1.13	1.074	0.262	4.1
				1.021	0.255	4.0
				0.944	0.315	3.0
				0.849	0.216	3.9
Exp. (b)	46.7	9.52	1.28	1.233	0.180	6.9
				1.189	0.191	6.2
				1.264	0.187	6.8
				1.226	0.173	7.1
Exp. (c)	47.5	10.91	1.15	1.104	0.177	6.2
				1.020	0.171	6.0
				1.003	0.182	5.5
				0.959	0.160	6.0
Exp. (d)	45.9	10.96	1.08	0.995	0.200	5.0
				0.975	0.200	4.9
				1.014	0.201	5.0